Send Orders of Reprints at reprints@benthamscience.net

Current Organic Chemistry, 2013, *17*, 000-000 1

Dendritic Chemistry Applied to the Construction of Tailored Functional Nanomaterials: Synthesis and Characterization of Gold Nanoparticle-Cored Dendrimers (NCDs)

Julieta I. Paez[a], Verónica Brunetti[b], Eduardo A. Coronado[c] and Miriam C. Strumia [a,*]

[a]*IMBIV-CONICET. Departamento de Química Orgánica. Facultad de Ciencias Químicas, Universidad Nacional de Córdoba. Haya de la Torre y Medina Allende. Ciudad Universitaria (X5000HUA). Córdoba, Argentina*

[b]*INFIQC-CONICET, Departamento de Fisicoquímica. Facultad de Ciencias Químicas, Universidad Nacional de Córdoba. Haya de la Torre y Medina Allende. Ciudad Universitaria (X5000HUA). Córdoba, Argentina*

[c]*INFIQC-CLCM-CONICET, Departamento de Fisicoquímica. Facultad de Ciencias Químicas, Universidad Nacional de Córdoba. Haya de la Torre y Medina Allende. Ciudad Universitaria (X5000HUA). Córdoba, Argentina*

Abstract: A family of Newkome-type dendritic molecules bearing a disulfide anchor group, different peripheral groups (-COOtBu or -COOH) and sizes or generations (Gn=0-2) was synthesized and used as ligand for the synthesis of gold nanoparticle-cored dendrimers (NCDs). These hybrid materials were characterized by means of UV-vis spectroscopy, TEM, and IR and NMR spectroscopies, finding that the capping molecules of the organic shell determine the solubility and stability of the different NCDs, as well as the characteristics of the inorganic core through a dendritic control characteristic for Newkome-type ligands. Remarkably, a combination of detailed IR and NMR studies allows for studying the ligand-ligand and ligand-core interactions that take place in these materials. It is demonstrated that concepts, techniques and methods normally used in organic and dendritic chemistry, such as the synthesis of precisely controlled architectures and their rigorous spectroscopic characterization, can be efficiently applied to engineer novel organic-inorganic hybrid materials with enhanced properties.

Keywords: Dendritic control, IR spectroscopy, nanoparticle-cored dendrimers, NMR spectroscopy, organic-inorganic hybrid nanomaterials, tailored properties.

1. INTRODUCTION

The development of hybrid organic-inorganic nanomaterials constitutes a multidisciplinary, exciting, rapidly evolving area of research. The combination of the rigidity, thermal stability, and the superior electronic, optical, and magnetic properties of inorganic frameworks with the structural diversity, flexibility, and processability of organic molecules has revealed new phenomena and properties not accessible from the individual components[1] and improved the existing functionality and performance.

Organic chemistry has played a very important role in this progress through the design, synthesis and characterization of constituting organic building blocks, advanced molecules able to control by themselves the whole hybrid material formation and properties. In particular, dendritic chemistry has contributed to this development by providing well-defined, monodisperse, functional macromolecular scaffolds, which rapidly access nanostructures through self-assembly fabrication methods [2,3]. The preparation of dendritic-inorganic hybrid nanocomposites evolved in the highly defined, controlled nanoparticle-cored dendrimers (NCDs), core-shell nanocomposites formed by an inorganic nanoparticle (NP, the core) positioned at the centre of the structure and an organic shell given by dendrons attached to the core in a radial way by specific interactions. When a certain density of dendritic wedges is attained, NCD structure is comparable to a dendrimer backbone since both feature defined and differentiable exterior, interior and void spaces (cavities) [4]. Moreover, the number and nature of the outermost functional groups determine the characteristic properties of these hybrid materials, like solubility, reactivity or permeability through the dendritic barrier [4,5]. In comparison to related hybrid nanomaterials, the synthesis of NCDs constitutes an important advance towards novel organized structures [4] provided their chemical and photochemical stability [6] and their predictable and precisely controlled structure. Additionally, functional NCDs are synthetically accessible by the introduction of redox, photochemical or catalytic moieties in a particular position.

One way to prepare NCDs is through the so-called direct method that comprises the simultaneous production of the inorganic core and its stabilization *via* attachment of dendrons having suitable moieties at the focal point [4]. This reaction is equivalent to the last step in a conventional, convergent, dendrimer synthesis [7]. It has been already shown that the information programmed into the dendritic branches directly controls the core characteristics, and offers the possibility of tuning its shape [8,9] and size [10-16]. This effect is called *dendritic control* and means that each dendritic chemical structure and generation (Gn) lead to a particular core.

Upon increase of structural complexity of the organic coating in hybrid materials, the need for more advanced and detailed characterization methods and techniques became imperative, since NCDs properties directly determine their application. In this context, the transfer of spectroscopic techniques traditionally used in organic chemistry, such as IR, NMR and UV-vis encouraged and supported the study of the new nanocomposites. Indeed, the

*Address correspondence to this author at the IMBIV-CONICET. Departamento de Química Orgánica. Facultad de Ciencias Químicas, Universidad Nacional de Córdoba. Haya de la Torre y Medina Allende. Ciudad Universitaria (X5000HUA). Córdoba, Argentina; Tel: 0054-351-4334170/73 ext 120; Fax: 0054-351-4334170/73 ext 151; E-mail: mcs@fcq.unc.edu.ar

1385-2728/13 $58.00+.00

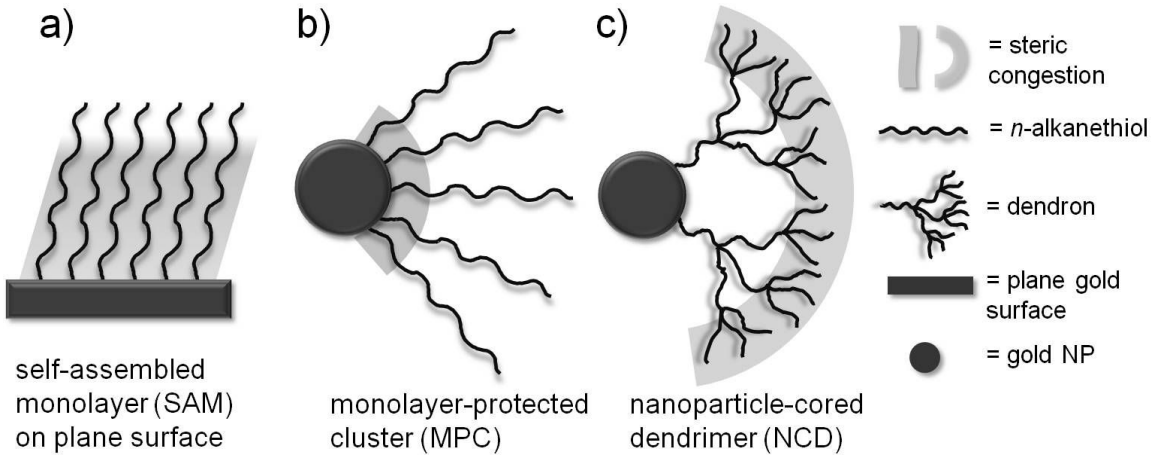

Scheme 1. Representation of the sterically congestioned regions in the organic coating of different hybrid inorganic-organic materials, (a) SAMs on a plane surface, (b) MPCs, and (c) NCDs.

characterization of NCDs was based on the previous findings reported for self-assembled monolayers (SAMs) and monolayer-protected clusters (MPCs), their simpler predecessor hybrids. It is known that the organic monolayer of these materials presents different structural features that lead to a different steric congestion in each particular case (Scheme **1**). In SAMs (a) formed by *n*-alkanethiols on a flat gold surface, the chains adopt a quasi-crystalline, almost completely extended structure mainly in a *trans*, *gauche*-free conformation [17,18]. Most of the molecule length presents steric congestion and a restricted mobility, except for the disordered, highly movable outermost chain segments that feature *gauche* defects [18]. In MPCs (b), the substrate curvature affects the packing efficiency among neighbor chains and leads to a radial, fan-like disposition of the ligand molecules. Thus, packing density decreases from the NP surface outwards whereas chain mobility increases in the same direction [17-19]. In NCDs (c), the substrate curvature effect takes place as well. The presence of dendrons instead of *n*-alkanethiols as ligands causes important differences in relation to MPCs, since dendrons are branched structures that are expected to adsorb with lower packing density than their corresponding linear analogues [20]. Thus, steric congestion along the monolayer also modifies. After dendron self-assembly on the surface, large void spaces remain near the metal core and the methylenes located close to the NP surface evidence a relatively low or null congestion [11]. In contrast to the tendency observed for MPCs, in NCDs the steric congestion may increase from the NP surface outwards.

Despite the use of the mentioned spectroscopic techniques made so far, further advance is needed to gain a more complete understanding of the disposition, organization and interactions played into the organic coating of hybrid materials, to extent their scope for new applications. Therefore, the high structural complexity of the coating layer demands more advanced and detailed characterization methods and techniques.

In this article we report on the synthesis of a family of Newkome-type dendritic molecules bearing a disulfide anchor group which are used as ligands for the synthesis of gold NCDs. The main structural differences considered in the coating molecules are the peripheral groups (-COOtBu or -COOH) and the molecular size or generation (Gn=0-2). The characterization of these dendritic-inorganic hybrid materials was performed by means of UV-vis spectroscopy, TEM, and especially, IR and NMR spectroscopies. The main focus of this work is evaluating the characteristics of the individual components of the hybrid and also the way they interact with each other, to gain a deeper insight into the dendritic control that can be attained in this kind of materials. We aim to demonstrate that concepts and techniques habitually employed in the organic and dendritic chemistry can be efficiently transferred to the design and study of tailored hybrid nanomaterials for new and enhanced applications.

2. EXPERIMENTAL PART

2.1. Materials

All reagents and solvents were used as received. Sodium tetrachloroaurate(III) hydrate and sodium borohydride were analytical grade and purchased from Sigma-Aldrich or Merck. Chloroform, absolute ethanol, and acetonitrile (HPLC grade) were acquired from Sintorgan. All solutions were prepared immediately before use. Ligand G0-COOH is commercial (Aldrich) and the synthesis of ligands G1-tBu and G1-COOH have already been published by our group [21]. Ligands G2-tBu and G2-COOH are new and their syntheses are described in the Supplementary Material section. Glassware and magnetic bars used for NCD synthesis were previously cleaned with sulfonitric mixture, washed thoroughly, and dried in the oven overnight.

2.2. Instrumentation and Measurements

NMR spectroscopy was performed on a *Bruker Avance II* (400.16 MHz, BBI probe, Z-gradient) spectrometer at 25 °C using $CDCl_3$ or methanol-d_4 (Aldrich) as solvents. The spectra were analyzed using TopSpin 2.0 or MestreC software. Chemical shifts (δ) were quoted in parts per million referenced to the solvent residual peak and coupling constants (*J*) in Hz. FT-IR measurements were carried out on a Nicolet-5SXC as the average of 32 scans at a resolution of 4 cm^{-1}. Samples were prepared by placing a drop of NCD solution over KBr pellets followed by the solvent evaporation at room temperature. The data were processed using the EZ Omnic E.S.P. 5.1 software. IR spectra are shown normalized in relation to the most intense band. UV-vis experiments were measured on a Shimadzu MultiSpect 1501 spectrometer between 300-800 nm at 25 °C. TEM images were obtained with a JEM 1200EXII-JEOL electron microscope operating at 80 kV. Samples for TEM were pre-

pared by drop-casting one drop of the colloid onto standard carbon-coated Formvar films copper grids (200-mesh), followed by the solvent natural evaporation. For each sample, at least four typical regions were scanned. The images were analyzed using the ImageJ software. The mean particle diameter and standard deviation were calculated by counting at least 300 particles from the enlarged photographs. Statistical analysis and plotting were carried out using OriginPro 8.0 and SigmaPlot 10.0 software.

2.3. GENERAL PROCEDURE FOR THE SYNTHESIS OF NCDS

A modified, one-phase strategy originally proposed by Smith's group[10] was followed. In a 5 mL glass test tube equipped with magnetic stirrer, tetrachloroaurate (3.3 μmol) and the corresponding disulfide ligand (1.6 μmol) were dissolved in EtOH (0.43 mL), obtaining a yellowish solution. Subsequently, sodium borohydride (6.5 μmol, 0.11 mL of freshly prepared 5.7 mM solution in EtOH) was rapidly added under vigorous stirring. The darkening of the solution was observed at once due to the formation of the NPs. After stirring the mixture for 30 min at room temperature, a stable colloidal system was obtained, which was characterized immediately.

Synthesis of NCD-G0-tBu

A reddish-brown colloid was obtained. **IR** ν_{max} = 3308*m* (NH), 2922- 2851*m* (ν CH), 1650*s*-1644*m* (Band I amide), 1556*m* (Band II amide), 1454-1362*m* (δ CH).

Synthesis of NCD-G1-tBu

Brown colloid. **IR** ν_{max} = 3334*m* (NH), 2977-2929*m* (ν CH), 1731*s* (C=O ester), 1655*m* (Band I amide), 1542*m* (Band II amide), 1457-1368*m* (δ CH), 1317*w* (Band III amide), 1154*s* (-CO_2- ester).

Synthesis of NCD-G2-tBu

Ruby red colloid. **IR** ν_{max} = 3321*m* (NH), 2978-2931*m* (ν CH), 1731*s* (C=O ester), 1655*m* (Band I amide), 1541*m* (Band II amide), 1457-1368*m* (δ CH), 1317*w* (Band III amide), 1156*s* (-CO_2- ester).

Synthesis of NCD-G0-COOH

Dark brown colloid. **IR** ν_{max} = 3399*m* (OH acid); 2959-2922*m* (ν CH); 1731-1708*s* (C=O acid), 1238*m*, 1185*m*.

Synthesis of NCD-G1-COOH

Reddish-brown colloid. **IR** ν_{max} = 3349*m* (OH acid), 3076*m* (NH), 2982-2941*m* (ν CH), 1731*s* (C=O acid), 1655*m* (Band I amide), 1556*m* (Band II amide), 1308*w* (Banda III amide), 1193*m* (-CO_2- acid).

Synthesis of NCD-G2-COOH

Ruby red colloid. **IR** ν_{max} = 3346*m* (OH acid), 3072*m* (NH), 2980-2940*m* (ν CH), 1731*s* (C=O acid), 1652*m* (Band I amide), 1556*m* (Band II amide), 1311*w* (Band III amide), 1190*m* (-CO_2- acid).

3. RESULTS AND DISCUSSION

3.1. Experimental Design

In this work, a family of aliphatic, Newkome-type molecules with a central disulfide moiety, different peripheral groups (-COOtBu and -COOH) and increasing sizes (G0 to G2) was first synthesized. Then, these molecules were used as ligands and stabilizers for the synthesis of NCDs following a one-phase methodology carried out in organic media. This procedure allows for the preparation of functionalized, templated, "clean" NPs, since no phase-transfer agents were needed. Disulfide groups are used as anchoring units to attach the ligand molecule on the gold surface, whereas the different terminal moieties and molecular sizes are expected to control the final properties of the colloidal systems like solubility or stability, through the variation of shell packing density or adsorbate-adsorbate interactions.

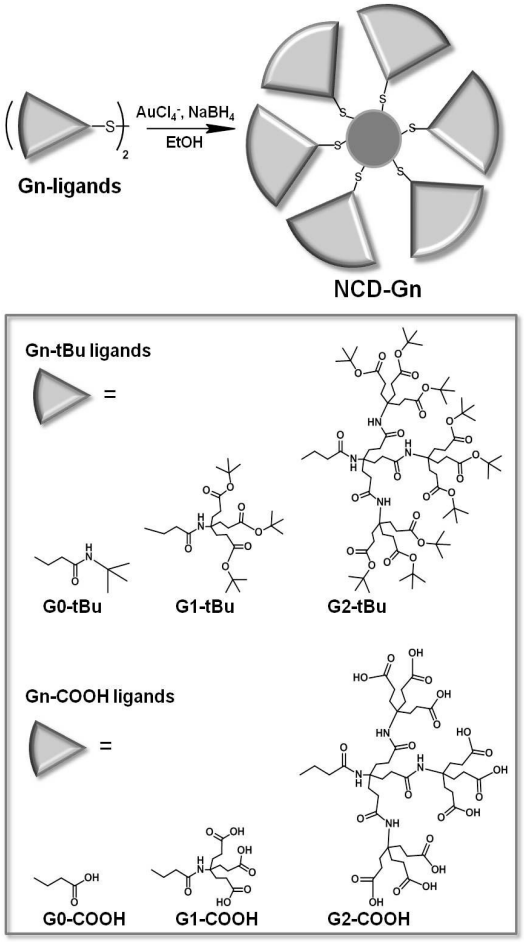

Scheme 2. Synthesis of NCDs and ligands used.

3.2. Synthesis of NCDs and Control Experiments. Colloidal Solubility and Stability

The synthesis of NCDs was conducted in ethanol, employing sodium borohydride as reductor of the gold precursor and avoiding the use of phase-transfer agents. In this process, the borohydride reduces $AuCl_4^-$ to metallic gold, and the formed NPs are immediately stabilized by the adsorption of the disulfide ligands present in the solution, as shown in Scheme **2** [22].

With the aim of compare the as-prepared NCDs with other Newkome-type NCDs previously reported [10], the synthesis was performed at room temperature and using a molar ratio of reductor/Au^{3+}/disulfide (4:2:1), maintaining an equimolar Au^{3+}/S ratio and an excess of reductor. Using the same conditions previously described, two different sets of control experiments were additionally carried out where the addition of one of the reagents was omitted. The first experiment consisted in the synthesis of NPs without the use of any stabilizing disulfide ligand, observing the formation

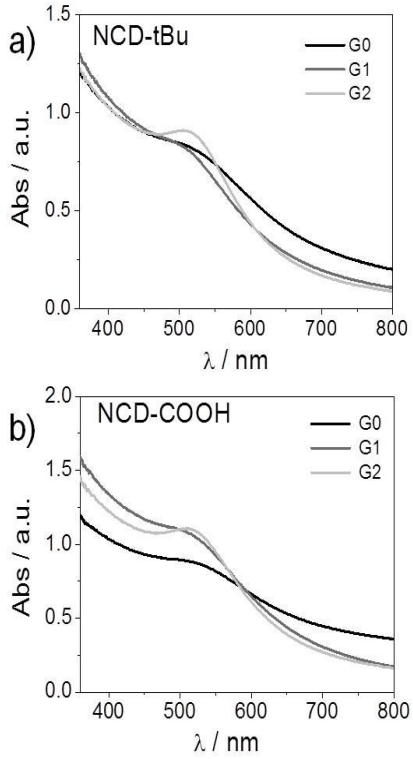

Fig. (1). UV-vis spectra (EtOH) of a) NCD-tBu and b) NCD-COOH.

of black NPs that aggregated and precipitated irreversibly within a few seconds, in agreement with previous studies [11,23]. Second, the absence of gold precursor was tested to evaluate the effect of the reductor on the pure ligands, observing by ^{1}H NMR (not shown) that the borohydride did not reduce any of their functional groups (disulfide, amino, ester, carboxylic acid) under these experimental conditions.

The characteristics of the resulting NCDs, such as solubility and stability, depended on the ligand used. The solubility of NCDs was similar to that shown by the pure ligands and depended on the peripheral groups of the molecule: NCD-tBu were soluble in most organic media like chlorinated solvents, alcohols or THF; whereas NCD-COOH were only soluble in polar organic solvents such as alcohols, THF or DMF.

The stability of the colloidal systems, in turn, was dependent on the generation of the coating ligand. NCDs-G0 were the most unstable ones and precipitation was observed within the first 48 h of synthesis. In contrast, NCDs-G1 and NCDs-G2 remained soluble and stable over several weeks when the precipitation of some NPs was observed, being possible to redisperse them by a few seconds of ultrasound. Surprisingly, NCDs-G1 were even more stable than NCDs-G2. Another issue related to colloidal stability was observed during solvent drying and redispersion over repetitive cycles. NCDs-G1 and NCDs-G2 could be dried and resolubilized in organic solvents several times without decomposition of aggregation, which is consistent with previous reports on NCDs [7,11]. In contrast, due to their instability, NCDs-G0 were stored as dried powders and only redispersed to perform the corresponding characterization studies.

3.3. UV-vis and TEM Characterization

NCDs were initially characterized by UV-vis and TEM means to determine the optical properties, size, and shape of NPs. UV-vis spectroscopy has been widely used for NP characterization and it is known that the intensity and position of the local surface plasmon resonance (LSPR) band of metallic NPs is strongly related to their size, shape, and environment [24]. Figure **1** shows the UV-vis spectra of NCD-tBu (a) and NCD-COOH (b). In all cases, only one LSPR band, with a considerable spectral broadening due to electron confinement effects (surface scattering) in the 500-520 nm wavelength range is observed. This LSPR broadening is characteristic of small, nearly spherical gold nanoparticles with a size below 5 nm [24]. Besides, an intensity and definition increase of the LSPR band indicates an increase of NP size. As this LSPR broadening increase as the size of the NP decreases, based on the experimental value of Full Width at Half Maximum (and assuming that the main source of signal attenuation is due to surface scattering), it could be anticipated that the size tendency of the NPs is: NCD-G2 > NCD-G0 ≥ NCD-G1.

TEM has also been proved to be an essential technique for an easy determination of the size of metal NPs [24]. The TEM micrographs of the NCDs and their corresponding histograms (Fig. **2**) show that the synthesized NPs are quasi-spherical and present a size below 5 nm, in good agreement with UV-vis results. Since TEM images also evidence a non-constant separation between NPs, the organic layer thickness cannot be estimated from the micrographs [11,23].

3.4. Dependence between Ligand and NP Size

As previously mentioned, the evaluation of the dendritic structure effect on NCD characteristics is an interesting issue. It is proposed that not only the size (generation) but also the chemical structure of the dendritic capping molecules define the properties of the hybrid material.

There have been observed different tendencies in the dendritic control over NP size. The first group involves NP size increase upon generation increase, for example NCDs prepared using Percec-[23,25] or Fréchet-type- [11,12], arenodendritic[16] or carbosilane dendritic molecules [26]. In a second group, NP size decreases upon generation increase, which is the case of dendritic disulfides based on L-lysine [14]. There is a third group where NP size does not show a clear continuous tendency with the dendritic generation, such as those prepared using some Fréchet-type dendrons [15,27]. There is also the case within a certain tendency where "jumps" in NP size are produced, especially upon high generation conditions since the entrapping mechanism becomes more important [11]. All these examples indicate that the dendritic size and backbone, the characteristics of the focal and ending groups, and the methodology of NCD preparation play a key role in the material final properties. Additionally, in general the NP size dispersity has not been shown to follow a clear tendency with ligand generation. Finally, it is important to mention that only a few works have reported the non-dendritic reference NCD-G0 [14,16].

In this work, two series of NCDs were prepared, NCD-tBu and NCD-COOH, obtaining in all cases quasy-spherical NPs. In both series, the calculated mean NP diameter seems to decrease from G0 to G1 and likely increases from G1 to G2, while standard deviation does not change notably (20-25%). This spherical shape and discontinuous size tendency is similar that the one informed by Love *et al.* for the synthesis of other NCDs using dendritic, Newkome-type disulfides having methylester peripheral groups [10]. As the three series (-COOMe, -COOtBu and -COOH) show the same tendency, the Newkome-type dendritic backbone (aliphatic, 1→3 branching motif) is likely to be the most relevant parameter in the

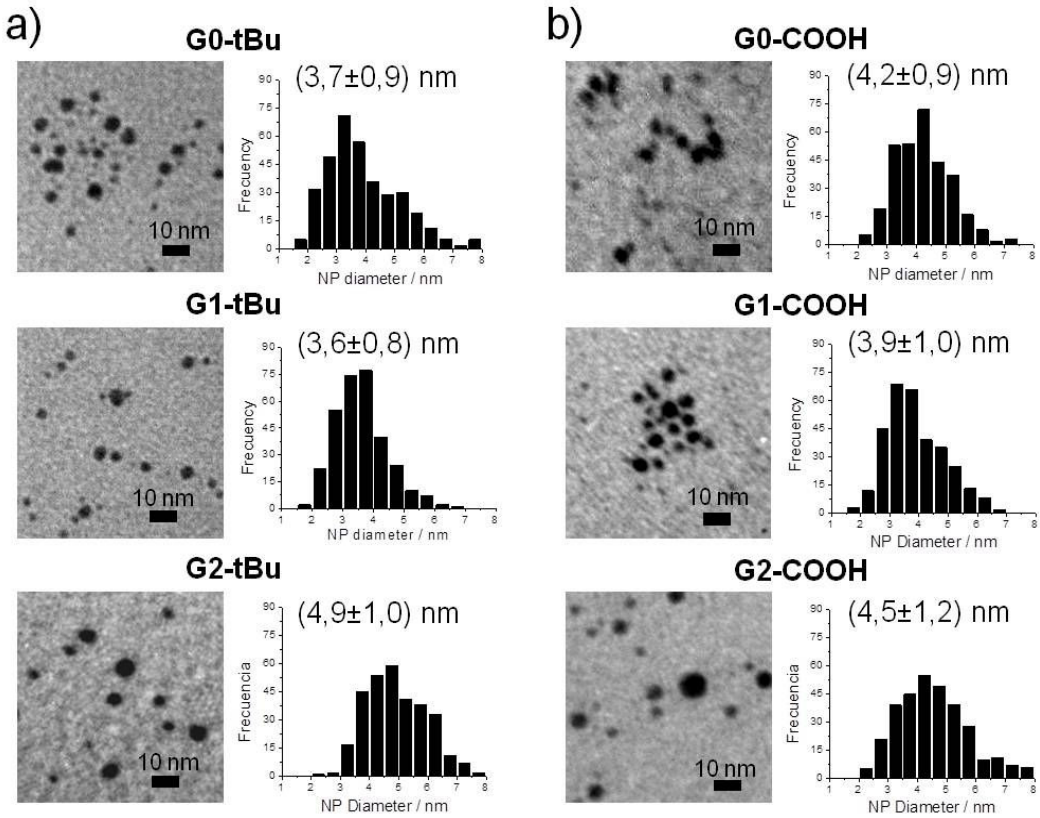

Fig. (2). TEM characterization of a) NCD-tBu and b) NCD-COOH.

dendritic control. Besides, the small difference in NP size from one series to others indicates that the terminal groups also influence NP size, albeit to a much lesser extent. Those differences might be related to the different ligand-ligand non-covalent interactions, either hydrophobic or *via* hydrogen bonds, that take place upon NP formation in each case.

3.5. IR Characterization

IR spectroscopy has been shown to be a valuable technique for the structural study of MPCs in terms of conformation, packing and lateral interactions of chains in the organic coating [24]. It also provides important information about whether different functional groups such as amino, amide, hydroxyl or carboxylic acids; that might be able to interact with the metal surface, effectively participate in the NP stabilization process [9,23,28,29]. The study of these hybrid materials *via* IR spectroscopy involves the comparison of the spectra of the corresponding ligand free and attached to the metal surface.

Although the helpfulness and versatility of this technique have been already successfully proven for the study of MPCs, it has been less used for NCD characterization [11]. Since in the latter case spectral complexity increases notably, the information that can be obtained is usually limited. In this context, IR spectroscopy has enabled to analyze the chemical change experimented by the ligands due to a redox-mediated adsorption process [9,15], as well as to follow subsequent chemical transformations of the adsorbed ligands after NP functionalization, such as the hydrolysis of the functional moieties located at the dendritic periphery [12]. In the present work, IR spectra were recorded over each free disulfide ligand and its corresponding NCD, both in the solid state since conformational order is higher [30], and then evaluated comparatively.

3.5.1. NCD-tBu

C-H vibrations

C-H stretching signals are particularly sensitive to conformational and environmental changes of alkylic chains, which traduces in an alteration of both frequency and wide band [30-32]. In a previous report, Porter *et al.* showed that linear alkylic disulfides adsorb onto a NP surface in an ordered and densely-packed fashion, leading to the narrowing and shifting to lower frequencies of C-H stretching bands in comparison to the pure disulfide [30]. Indeed, among C-H stretching signals, $\nu_{as}CH_2$ has been reported to be especially sensitive to chain packing, since located at 2818 cm^{-1} is indicative of dense packing whereas at >2922 cm^{-1} it points out to poorly packed chains [20].

Figure **3** depicts the IR spectra of the pure ligands and their corresponding NCDs, which most intense vibrations are assigned in detail in Table **1**. Gn-tBu disulfides present two types of C-H groups, $-CH_3$ from -tBu peripheral moieties and $-CH_2-$ from internal chains. In relation to its precursor G0-tBu (spectrum a), NCD-G0-tBu (b) shows the noticeable shift of stretching C-H bands to lower frequencies (-46 and -79 cm^{-1}) and the increase of their relative intensity. A similar trend is observed when G1-tBu (c) and NCD-G1-tBu (d) spectra are compared, since in the latter the signal corresponding to the $\nu_{as}CH_2$ mode appear slightly shifted to lower frequency (-6 cm^{-1}) and increased in intensity, while the other bands remain almost unaffected. Finally, the stretching bands observed for G2-tBu (e) are present and practically unaltered (within experimental error) in the spectrum of NCD-G2-tBu (f).

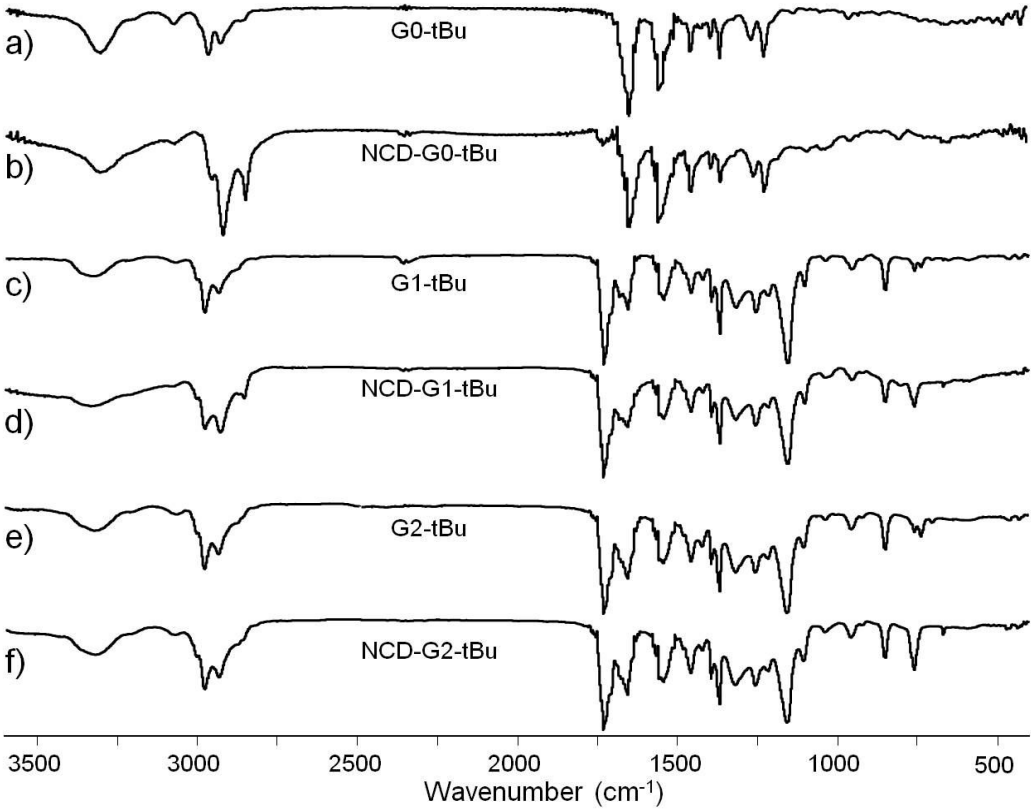

Fig. (3). Normalized IR spectra of pure Gn-tBu (a, c, e) and their corresponding NCD-tBu (b, d, f).

The results indicate that, as a consequence of the interaction with the metal, some conformational changes on Gn-tBu ligands occur and the C-H stretching vibrations of NCD-tBu appear affected, compared to the signals of the corresponding free ligands [9,12,33]. This process leads to both shift of C-H stretching bands to lower frequencies and intensity band increase, indicating the ordering and packing of the alkylic chains in the monolayer. Interestingly, this effect depends on the ligand generation as it is notable for G0, moderate for G1 and practically null for G2. This feature denotes that the smallest and movable G0 is able to pack densely, hence giving highly ordered, compact monolayers. In contrast, monolayers generated from G1 and G2 are less ordered and packed, given the higher molecular bulkiness which hinders the ligand packing. It is important to note that the increase of signal intensity can only be attributed to this phenomenon and not to the presence of impurities derived from the use of phase transfer agents, as previously reported [12]. Note that no band widening was observed in C-H stretching bands.

Hydrogen Bonding Interactions

IR spectroscopy has also been employed to study the strength of hydrogen bonding interactions among chains in a monolayer, since these forces directly influence SAM stability [20,32].

G0-tBu (a) presents the characteristic amide signals like N-H stretching, Band I (corresponding mainly to C=O stretching with a small N-C=O bending contribution) and Band II (which involves mainly N-H bending with a small C-N stretching contribution) [34,35]. The corresponding NCD-G0 shows these bands as well with no noticeable changes in frequency or intensity. G1-tBu presents the stretching C=O band of the ester moiety plus the signals corresponding to amide groups like N-H stretching, Band I, Band II, and Band III. The latter is associated to the in-phase combination of N-H stretching and C-N stretching modes [36]. In comparison to its precursor, NCD-G1 spectrum shows a very similar picture with a small difference given by the slight shift of the N-H stretching band to a higher frequency (+9 cm^{-1}). Lastly, G2-tBu depicts the same amide and ester vibrations previously specified which remain practically unaffected after in NCD-G2. In this spectra series, the amide signals observed are consistent with secondary, hydrogen-bonded amide moieties, mainly present in their *trans* conformation [35].

The results indicate that the mentioned hydrogen-bond interactions remain practically unaffected in NCDs, except in NCD-G1 where they appear slightly weakened. The general non-modification of ester and amide vibrations after ligand adsorption indicates that those groups do not interact directly with the NP surface. This feature, together with TEM studies that show large NP sizes obtained in comparison to the relatively small disulfide molecular lengths, suggest that NP stabilization *via* an entrapment mechanism (the so-called dendritic box effect) can be ruled out, i.e. the lower generation ligands do not provide sufficiently large cavities to encapsulate NPs within their interior [37].

3.5.2. NCD-COOH

C-H Vibrations

Figure **4** displays IR spectra of the pure Gn-COOH ligands and their corresponding NCDs, which most intense vibrations are listed in Table **2**. These ligands present only one kind of C-H moieties given by the $-CH_2-$ groups of internal chains, thus the observed C-H bands correspond exclusively to methylene vibrational modes. Although Gn-COOH and NCD-COOH present weak, poorly defined C-H stretching bands, it is still possible to distinguish two signals located at around 2960 and 2925 cm^{-1}; these frequencies are higher than those expected for the $\nu_{as}CH_2$ and ν_sCH_2 modes, normally situated at 2926 and 2853 cm^{-1}, respectively [38].

Table 1. Assignation of the Main IR Vibrational Frequencies of Gn-COOH and NCDs-COOH In Solid State

	Vibrational Frequencies of Different Functional Groups (cm^{-1})						
	C-H stretching		Ester	Amide			
X-tBu	$\nu_{as}CH_3$	$\nu_{as}CH_2$	$\nu C{=}O$	$\nu N{-}H$	*Band I*	*Band II*	*Band III*
G0	2968	2930	--	3306	1649	1556	--
NCD-G0	2922	2851	--	3308	1650	1556	--
G1	2978	2935	1731	3325	1655	1542	1317
NCD-G1	2977	2929	1731	3334	1655	1542	1317
G2	2978	2935	1731	3323	1655	1542	1317
NCD-G2	2978	2931	1731	3321	1655	1541	1317

ν = stretching frequencies

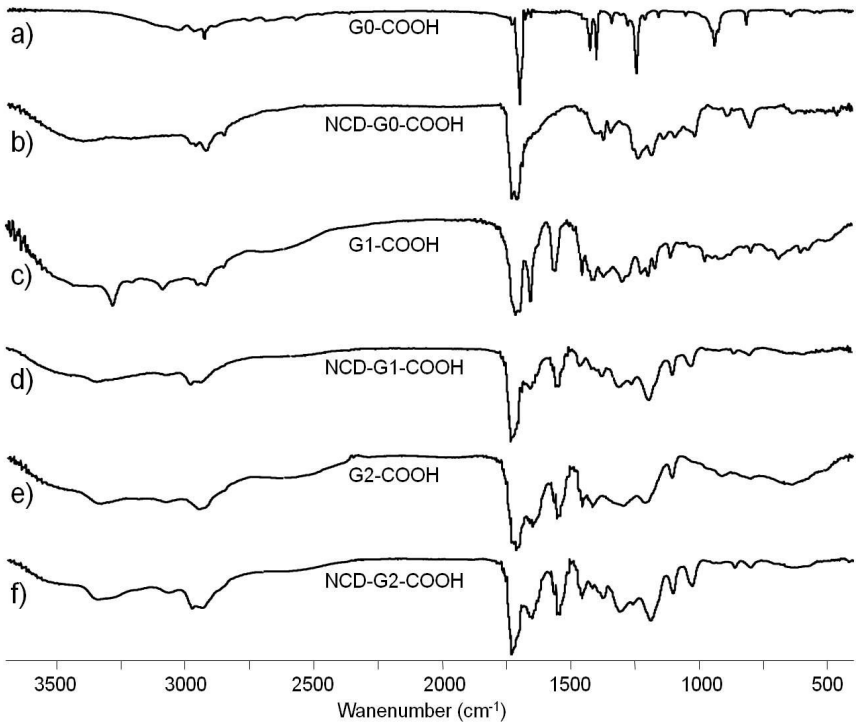

Fig. (4). Normalized IR spectra of pure Gn-COOH (a, c, e) and their corresponding NCD-COOH (b, d, f).

The stretching C-H bands observed in G0-COOH spectrum (a) are also seen in NCD-G0-COOH (b) albeit widened, slightly more intense, and shifted to lower frequencies (-9 and -6 cm^{-1}); feature associated with an ordering or packing of alkylic chains in the NP coating. Pure G1-COOH (c) shows C-H stretching bands that surprisingly, appear widened, slightly more intense, and shifted to higher frequencies (+27 and +17 cm^{-1}) in the corresponding NCD-G1 (d). The same evidence is observed for G2-COOH (e) and NCD-G2 (f), since in this couple C-H stretching bands are shifted +29 and +14 cm^{-1}. Such band shift to higher frequencies could be explained first in terms of a disorder increment of alkylic chains in relation to the free G1 and G2 ligands. However, it is also possible that this result indicates a strain increment over methylene groups, resembling the effect observed for strained methylene moieties in cycloalkanes [38]. It is well-known that strained methylenes, such as those in cyclopropane rings, present C-H stretching modes located at higher frequencies than the corresponding unstrained linear analogues [38].

Hydrogen Bonding Interactions

Peripheral carboxylic acid moieties, present in both Gn- and NCD-COOHs are able to establish hydrogen bonding interactions. Indeed, all Gn-COOH spectra show O-H and C=O stretching bands associated with hydrogen bonded carboxylic acid groups [38]. Such bands shift to higher frequencies in all the corresponding NCDs, in NCD-G0 they move +371 and +30 cm^{-1} (together with the widening of the C=O stretching band), in NCD-G1 +62 and +26 cm^{-1}, and in NCD-G2 are shifted +10 y +9 cm^{-1}, respectively. These observations indicate a weakening of hydrogen bonds along -COOH groups of NCDs in relation to the free Gn-COOHs.

G1-COOH and G2-COOH also have internal amide moieties. Their corresponding spectra present N-H stretching, Band I, and

Table 2. Assignation of the Main IR Vibrational Frequencies of Gn-tBu and NCDs-tBu In Solid State

	Vibrational Frequencies of Different Functional groups (cm^{-1})							
	C-H Stretching		Carboxylic Acid		Amide			
X-COOH	$\nu_{as}CH_2$	ν_sCH_2	*ν O-H*	*ν C=O*	*ν N-H*	*Band I*	*Band II*	*Band III*
G0	2968	2928	3028	1699	--	--	--	--
NCD-G0	2959	2922	3399	1731-1708	--	--	--	--
G1	2955	2924	3287	1713-1696	3092	1654	1559	--
NCD-G1	2982	2941	3349	1731	3076	1655	1556	1308
G2	2951	2926	3336	1730-1714	3078	1651	1556	--
NCD-G2	2980	2940	3346	1731	3072	1652	1556	1311

ν = stretching frequencies

Band II vibrations coincident with the assignation of secondary, hydrogen bonded amides, mainly in the *trans* conformation [35]. In comparison, NCD-G1 spectrum shows the shifting of the N-H stretching band at lower frequency (-16 cm^{-1}), a notable decrease of Band I and Band II intensities, and the appearance of Band III. NCD-G2 shows the shifting of N-H stretching band at lower frequency as well (-6 cm^{-1}) and the appearance of Band III, although Band I and II remain practically unaffected. These results indicate that amide groups form stronger hydrogen bond interactions in their corresponding NCDs than in the free Gn-COOH, being this difference more evident for the G1/NCD-G1 couple.

3.6. NMR Characterization

In a similar way to IR, NMR spectroscopy has also been used to characterize MPCs, especially to gain information regarding the conformation of the alkylic chains in the organic monolayer [19,24,30,39,40]. The ^1H and ^{13}C one-dimensional techniques have been the most employed ones, since in MPCs the proton and carbon signals located in the sterically highly-congested region (see Scheme 1) are characteristically widened in comparison to the pure alkanethiols [24]. This effect depends on both the average packing degree and on the local mobility, i.e. it depends on the distance to the NP surface [41]. Manifold reasons have been proposed to explain such spectral widening. The methylene groups situated close to the NP surface present less mobility and experience faster spin relaxations due to dipolar interactions; accordingly, their signals appear widened [11,19,24,40,41]. In contrast, the methylene moieties located far away from the metallic core have higher freedom of movement, like in a liquid, and thus their spin relaxations are similar to the pure dissolved species, thus evidencing low or null widening [11,19,24,40,41]. Although this feature has been indicated as the main cause that leads to signal widening, others explanations have also been given, like the possible distribution of chemical shifts due to the heterogeneity of the Au-S anchoring sites on the NP (terraces, edges, vertexes) or due to spin-spin relaxation (T_2) [24].

The first pioneering studies about NCD characterization *via* NMR predicted that, if signal widening in MPCs was mainly based on the solid-like packing of ligands close to NP surface, this effect might be absent in NCDs. Or, in case of signal widening and inversely to MPCs, such effect might be associated to the NMR signals of the NCD-outermost functional groups, where steric congestion occurs [11]. However, as judged from different reports in the literature it seems to be rather more complicated to predict whether spectral widening would take place and where. For example, Gopidas *et al.* [11,12] reported in their NCD spectra a slight base-widening of the signal corresponding to the outermost protons, although ^{13}C NMR studies did not show this effect, feature that was explained on the basis of a lack of dense packing at that particular level of the monolayer. Deng *et al.* also reported signal broadening in thiophene NCDs [7]. Moreover, Shon *et al.* [42] published the widening of all signals in NCDs prepared by a convergent pathway, effect that also showed to be dependent on the dendron generation used as ligand. Additionally, Love *et al.* [10] found a slight widening of all proton signals in their NCD spectra, but especially in those signals corresponding to the moieties situated next to the NP surface. Finally, Ratheesh Kumar and Gopidas [15] observed proton signal widening for those nuclei closer to the metallic core in G1-NCDs, but the absence of this effect for higher-generation NCDs. All these examples evidence the complexity of NCD characterization by NMR means, and highlight the importance of a detailed analysis in combination with other spectroscopic techniques.

3.6.1. NCD-tBu

Figure **5** depicts the ^1H spectra of the pure Gn-tBu (a,c,e) and their corresponding NCDs (b,d,f). For pure ligands, the spectral region between 3.2-1.8 ppm shows the following signals: i) 3.1-2.4 ppm, the methylenes next to the disulfide moiety and ii) 2.3-1.8 ppm, the methylenes of the dendritic chains (absent in G0). Additionally, the complete spectra also show the methyls of the peripheral -tBu groups at 1.5-1.3 ppm and the amide NH at 6.20-5.70 ppm (see Supplementary Material section). Clearly, after the adsorption on the NP surface neither the chemical shift nor the multiplicity of these previously existing signals are largely modified. Surprisingly, for NCD-G0 (b) and NCD-G1 (d) it is also observed the appearance of up- and down-field "sister" signals of the triplets assigned as the methylenes closest to the NP (labeled with arrows in Fig. **5**). The realization of control experiments shows that, effectively, those new signals correspond to the NCDs themselves and are not due to side-products formed from the reduction of the disulfides (see section 3.2). To the best of our knowledge, this result has not been previously reported in the literature. To gain a deeper insight into these new signals, two-dimensional homo (COSY) and heteronuclear (HSQC and HMBC) NMR correlation studies were performed. The results (not shown) confirm that these extra signals

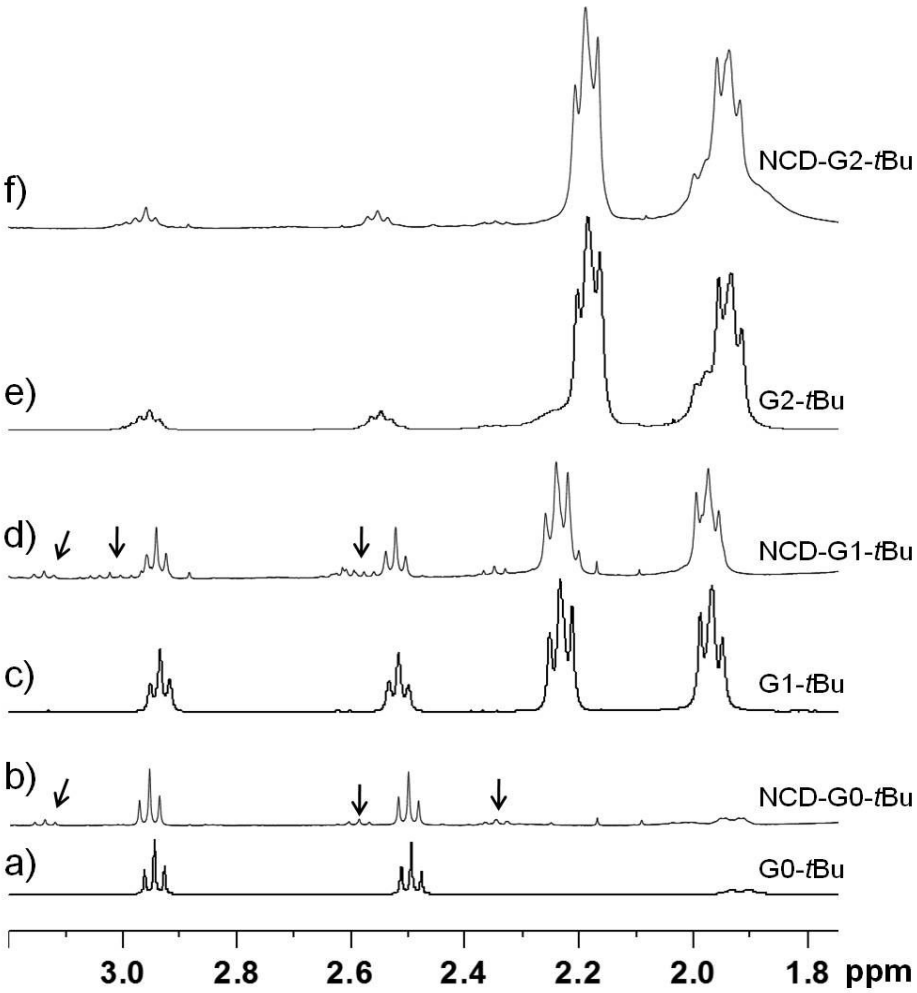

Fig. (5). ^{1}H-NMR spectra of free Gn-tBu and their corresponding NCD-tBu in $CDCl_3$ solution in the 3.2-1.8 ppm region. Important secondary signals are indicated by arrows.

correspond to the same Gn-tBu molecules interacting with the NP surface. In other words, in the hybrid most of the ligand molecules have a chemical environment that is similar to the free molecules in solution but a minor proportion of these ligands have a different one, probably because these molecules interact with different sites of the metal surface, such as terraces, edges or vortexes [19,24]. Apparently, NCD-G2 spectrum (f) does not show the same feature but, it is important to remark, the mentioned signals appeared already wide in the spectrum of free G2-tBu (e), thus hindering the observation of this effect. No significant differences in the NH amide signal were observed for the Gn/NCD couples.

With the aim to determine whether the proton spectra are sensitive to the steric congestion that NCDs are supposed to experience in the outermost region of the coating, the signals corresponding to the terminal -tBu groups (located at ca 1.4 ppm, spectra not shown) were compared. In all cases a slight base-widening of this signal was observed for NCD spectra in relation to free ligands, confirming the prediction that in NCDs the steric congestion increments at the periphery [11]. As the involved signals are singlets no further information could be obtained, which would have been the case if those signals presented another multiplicity. For example, Love *et al.* [14] reported on NCDs having terminal alkenes groups, whose proton signals were used as probes to describe the chain conformation. Taking advantage of the clear multiplicity of alkene protons, a better signal definition was related to a higher mobility of these moieties.

^{13}C spectra of NCD-G1 and NCD-G2 (Figs. **S7** and **S8**, respectively; on Supplementary Material) also show the widening of all signals in relation to the free ligands. This effect depends on the distance to the metal core as well, being particularly notable for those carbon nuclei situated next to it. Indeed, the signal associated to the -SCH_2CH_2- carbons (at *ca.* 37-33 ppm) is so largely widened that even seems to vanish and merge into the background. These results are in good agreement with previous studies carried out over MPCs [19,24] and NCDs [10] and strongly suggest that the Gn-tBu ligands are attached onto the NP through the interaction of the disulfide moiety with the gold surface.

It is important to mention that the ^{13}C spectra of NCD-G0 could not be acquired due to the low organic content and the instability of the colloidal sample.

At this point, it is necessary to emphasize that NMR and IR characterization are consistent and complementary to each other. IR results showed that after NP adsorption only C-H stretching vibration bands were altered whereas amide and ester bands remain practically unaffected, meaning that they unlikely interact with the metal surface. Instead, the proximity of the -SCH_2CH_2- moiety to the surface was revealed by NMR spectroscopy. Therefore, combining the results obtained, it is proposed that NCD-tBu present a

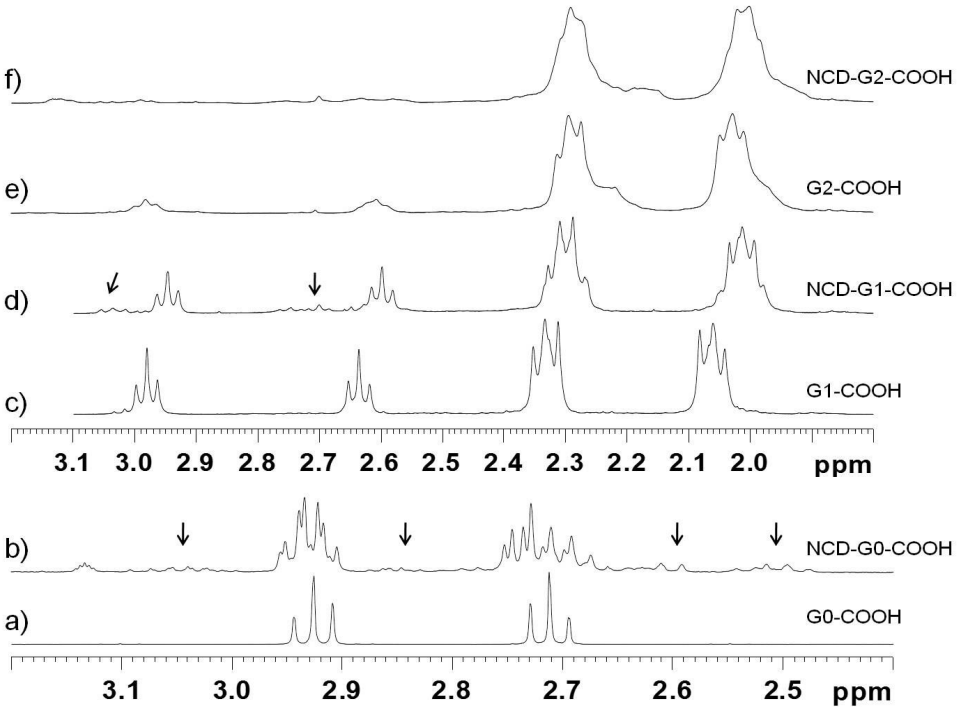

Fig. (6). ^{1}H-NMR spectra of free Gn-COOH and their corresponding NCD-COOH in methanol-d_4 solution (a-b) in the 3.2-2.4 ppm region; (c-f) in the 3.2-1.8 ppm region. Important secondary signals are indicated by arrows.

S-Au-based stabilization mechanism where the ligand interact with the NP surface *via* the disulfide moiety and the rest of the molecule is located in a radial way.

3.6.2. NCD-COOH

As Figure **6** illustrates, the spectra of pure Gn-COOH (a,c,e) in the 3.2-1.8 ppm region shows the following signals: i) 3.1-2.5 ppm, the methylenes of the -SCH_2CH_2- fragment, and ii) 2.4-1.9 ppm, the methylenes of the dendritic chains (absent in G0). These signals appear significantly altered in NCDs spectra (b,d,f) as a consequence of ligand-metal interaction adsorption. Importantly, such changes are not due to side products of ligand reduction, as proven by control experiments. NCD-G0 spectrum (b) shows the notable change in the multiplicity of the two methylenes signals next to the sulfur atom from triplets to multiplets, together with the appearance of up- and down-field "sister" signals (indicated with arrows in the Figure) which, as said before, can be ascribed to the interaction of the ligands with different sites of the NP [19,24]. In turn, NCD-G1 (d) shows the presence of such "sister" signals of the central -SCH_2CH_2-moiety as well, alongside the widening, up-field shifting and changing of multiplicity of the methylenes ascribed to the dendritic chains. In NCD-G2 (f), all signals appear deformed and widened to such an extent that their multiplicity can no longer be distinguished [39]. Signal widening of the dendritic methylenes may indicate that those groups present lower mobility in the NCDs than in the pure Gn-COOH. Additionally, two-dimensional correlation measurements (COSY, HSBC, and HSQC; not shown) also confirmed that the mentioned signals belong to molecules of ligand interacting with the NP core.

^{13}C spectra of NCD-G1 and NCD-G2 (see Supplementary Material, Figs. **S9** and **S10**) evidence the widening of all carbon signals in relation to free ligands, especially those of the -SCH_2CH_2- fragment suggesting its proximity to the NP surface. Surprisingly, the carbonyl of the terminal acid moieties appears vanished as well. This last feature indicates that those -COOH groups might also be involved in the shell stabilization *via* interactions with the NP surface, especially in NCD-G1 and less notably in NCD-G2. A similar behavior was recently suggested by Pérez *et al.* for gold NPs coated with peptide molecules containing -COOH and thioether groups [43].

The combined analysis of NMR and IR results offers a more complete picture. IR studies showed for NCD-G1 and NCD-G2 the shifting of C-H stretching signals at higher frequencies, the weakening of acid- and the reinforcing of amide-hydrogen bonds in relation to the free ligands. NMR results indicated the proximity of the -SCH_2CH_2- fragment to the surface and suggested that the peripheral -COOH groups may also be located somewhere close to the metal core and participate in the ligand-core interactions. A possible explanation to these results would be the occurrence of both disulfide/Au and -COOH/Au interactions. For this purpose, the ligand would first adsorb onto NPs through S-Au interactions, and then the dendritic chains would bend and fold to the metal surface to promote acid-gold interactions. This feature would explain the weakening of hydrogen bonding among -COOH groups (since they now would interact with the NP core), and also the shifting of the C-H stretching vibrations to higher frequencies due to an increment of either the disorder or the strain among alkylic chains. Thus, it is proposed that NCD-COOHs present mainly S-Au interactions, together with some acid-Au interactions.

3.7. Effect of the Reaction Conditions on the NP Size

Aside from the capping ligand architecture, the characteristics of the resulting NP core in both MPCs and NCDs also depend on a broad number of experimental parameters, like the molar ratio between gold precursor/ligand/reductor [24,44], reductor type [45], temperature [24], reductor addition rate [23,24], among others.

Although the effect of the reaction conditions on the NP size has been widely explored for MPCs[24,46] this is not the case for NCDs. As far as we know, there is only one report from Jiang et al

Table 3. Mean NP Diameter of Newkome-type NCDs Synthesized Following the same One-Phase Methodology But Under Diverse Reductor/Gold Ratio and Temperature Conditions, and Using Ligands with Different Generations and Terminal Groups.

NCD Series		Reference NCDs[a]		NCD-*t*Bu		
Ligand Peripheral Groups		-CO_2Me	-CO_2tBu	-CO_2tBu	-CO_2tBu	
conditions	red/Au[b]	(10:1)	(10:1)	(5:1)	(2:1)	(2:1)
	temp.	r.t.[c]	r.t.	r.t.	r.t.	0 °C
Gn[d]	G0	--	3,7±1,4	3,7±1,1	3,7±0,9	4,3±1,0
	G1	2,4±0,5	--	2,9±0,8	3,6±0,8	3,5±0,9
	G2	2,6±0,5	--	3,9±1,2	4,9±1,0	5,7±1,5

[a] data taken from reference [10]; [b] reductor/Au^{3+} molar ratio; [c] room temperature (25 °C); [d] ligand generation. Shadowed cells: results of the present work

where the effect of molar ratio between reductor/gold precursor on NP size was studied [23].

The NP sizes informed in Figure **2** correspond to NCDs synthesized at room temperature and using a molar ratio of reductor/Au^{3+}/disulfide (4:2:1), where a reductor excess is present. With the aim to get a deeper insight into the importance of the different experimental parameters on NCD synthesis, other reaction conditions were explored using NCD-tBu as a model system (see Table **3**). First, the reductor ratio was increased 2.5 and 5 times, keeping constant the other parameters. The 2.5-fold increase of reductor concentration afforded in general smaller NPs, whereas the 5-fold increase led to the formation of instable NCDs that precipitated in a few minutes. This last result observed for a very high concentration of reductor is in good agreement with previous studies that highlighted the convenience of using an intermediate reductor/Au^{3+} ratio, since at very low of very high values instable NPs are produced [44]. Second, while maintaining the initial reductor/Au^{3+}/disulfide molar ratio of (4:2:1), the reaction temperature was decreased to 0 °C, observing generally in such case the formation of bigger NPs. Previous studies showed that NP size depends on the "reductor power" of the initial mixture; a higher reductor power leads to the synthesis of smaller NPs. This effect is achieved either using a more powerful reductor [23,45], or through the increase of the reductor/Au^{3+} molar ratio [23] (for example, upon increase of the reductor concentration) or incrementing the reaction temperature, as in the present case. As Table **3** shows, NCD-G0 is poorly sensitive to the reductor ratio but sensitive to the reaction temperature, NCD-G1 is poorly sensitive to temperature variation but sensitive to reductor concentration, and NCD-G2 in sensitive to the variation of both conditions. This behavior remarks the importance of the careful election of the working parameters. Moreover, the fact that under different reaction conditions the size tendency is the same also confirms the Newkome-type dendritic control.

At variance with the reference article where the use of dendritic disulfides afforded NPs with a lower size dispersity [10], in the present work such tendency was not observed. However, it is surprising that both NCD-G1-tBu and NCD-G1-COOH were the colloids with lowest dispersity in each series and that, coincidentally, both NCD-G1 were also the most stable systems.

3.8. Final Comments on the Importance of the Proper Selection of NCD Capping Molecules

The results obtained so far indicate that the synthesis of Newkome-type NCDs presents a particular kind of dendritic control in which NP size seems to decrease from G0-G1 and likely increases from G1-G2. Colloidal solubility and stability show to be dependent on the ligand used as well. The higher stability of NCDs-G1 and NCDs-G2 in relation to NCDs-G0 may be explained considering the low ordering and packing of dendritic ligands (G1 and G2) on the NP surface that enable higher molecular mobility and a better solvation of the organic coating and lead to a higher colloidal stability. Naturally, the next questions would be how this dendritic control can be exploited or which dendritic capping molecule is the most suitable one for the synthesis of functionalized NPs. Of course, the answer to these questions depends on the purpose they were designed for.

As mentioned before, the election of a particular dendritic ligand can be oriented to template NP synthesis in such a way as to control the metallic core, the organic layer and/or the colloidal macroscopic properties. For example, the selection of G2 as capping molecule allows for templating NP sizes in a wide range by adjusting simple experimental conditions; whereas if low-dispersed NPs are targeted, G1 would be the molecule of choice. Moreover, G1 would also be the most suitable capping agent if one is interested in preparing long-term stable NCDs, able to remain unaltered in solution for several months.

Finally, it is known from the literature that NCDs meant to be applied in catalysis require as much non-passivated metallic surface as possible, fact that is controlled by the different characteristics of the organic monolayer like dendritic molecular volume or packing density [47]. Although this feature has not been studied in this work, it is possible that the selection of either G1 or G2 as capping ligands would lead to NCDs active for catalysis, given their high molecular size and their lower packing density in the hybrids.

4. CONCLUSION

In this work, a family of Newkome-type disulfide molecules with different peripheral functionality and increasing size has been synthesized and used to prepare two series of gold NCDs. It was found that the capping molecules that form the organic shell determine the solubility and stability of the different NCDs, as well as the characteristics of the inorganic core through a dendritic control which is characteristic of Newkome-type ligands. These results highlight the role of dendritic chemistry in the precisely controlled engineering of these hybrid materials. Additionally, it was demonstrated that a detailed spectroscopic characterization of the resulting NCDs by a combination of IR and NMR spectroscopies, normally employed in both organic and dendritic chemistry, enables the study of the ligand-ligand and ligand-core interactions. In summary,

it was proven that concepts, techniques and methods normally used in organic and dendritic chemistry can be successfully transferred to create novel organic-inorganic hybrid materials with enhanced properties.

CONFLICT OF INTEREST

The author(s) confirm that this article content has no conflict of interest.

ACKNOWLEDGEMENTS

The authors thank Dr. Gloria Bonetto and Dr. Claudia Nome for their technical assistance with NMR and TEM measurements, respectively. Financial support from CONICET, ANPCyT, and SECYT-UNC is gratefully acknowledged. J.I.P. thanks CONICET for the fellowship provided.

SUPPLEMENTARY MATERIAL

Supplementary material is available on the publishers Web site along with the published article.

REFERENCES

[1] Heulings; Huang, X.; Li, J.; Yuen, T.; Lin, C. L. Mn-Substituted Inorganic-Organic Hybrid Materials Based on ZnSe: Nanostructures That May Lead to Magnetic Semiconductors with a Strong Quantum Confinement Effect. *Nano Letters,* **2001**, *1*, 521-525.

[2] Grayson, S. M.; Fréchet, J. M. J. Convergent dendrons and dendrimers: From synthesis to applications. *Chemical Reviews,* **2001**, *101*, 3819-3867.

[3] Smith, D. K.; Hirst, A. R.; Love, C. S.; Hardy, J. G.; Brignell, S. V.; Huang, B. Self-assembly using dendritic building blocks - Towards controllable nanomaterials. *Progress in Polymer Science,* **2005**, *30*, 220.

[4] Shon, Y.-S. In *Advanced Nanomaterials*; Geckeler, K. E., Nishide, H., Eds.; WILEY-VCH Verlag GmbH & Co. KGaA: Weinheim, Germany, 2010; pp 743-766.

[5] Paez, J. I.; Martinelli, M.; Brunetti, V.; Strumia, M. Dendronization: a useful synthetic strategy to prepare multifunctional materials. *Polymers,* **2012**, *4*, 355-395.

[6] Wang, Y. A.; Li, J. J.; Chen, H.; Peng, X. Stabilization of inorganic nanocrystals by organic dendrons. *Journal of the American Chemical Society,* **2002**, *124*, 2293.

[7] Deng, S.; Fulghum, T. M.; Krueger, G.; Patton, D.; Park, J.-Y.; Advincula, R. C. Hybrid Gold-Nanoparticle-Cored Conjugated Thiophene Dendrimers: Synthesis, Characterization, and Energy-Transfer Studies. *Chemistry – A European Journal,* **2011**, *17*, 8929-8940.

[8] Jiang, G.; Wang, L.; Chen, W. Studies on the preparation and characterization of gold nanoparticles protected by dendrons. *Materials Letters,* **2007**, *61*, 278.

[9] Palui, G.; Ray, S.; Banerjee, A. Synthesis of multiple shaped gold nanoparticles using wet chemical method by different dendritic peptides at room temperature. *Journal of Materials Chemistry,* **2009**, *19*, 3457-3468.

[10] Love, C. S.; Ashworth, I.; Brennan, C.; Chechik, V.; Smith, D. K. Dendron-protected Au nanoparticles-Effect of dendritic structure on chemical stability. *Journal of Colloid and Interface Science,* **2006**, *302*, 178.

[11] Gopidas, K. R.; Whitesell, J. K.; Fox, M. A. Nanoparticle-cored dendrimers: Synthesis and characterization. *Journal of the American Chemical Society,* **2003**, *125*, 6491.

[12] Gopidas, K. R.; Whitesell, J. K.; Fox, M. A. Metal-Core-Organic Shell Dendrimers as Unimolecular Micelles. *Journal of the American Chemical Society,* **2003**, *125*, 14168.

[13] Love, C. S.; Chechik, V.; Smith, D. K.; Brennan, C. Dendron-stabilised gold nanoparticles: Generation dependence of core size and thermal stability. *Journal of Materials Chemistry,* **2004**, *14*, 919.

[14] Love, C. S.; Ashworth, I.; Brennan, C.; Chechik, V.; Smith, D. K. Dendritic nanoparticles - the impact of ligand cross-linking on nanocore stability. *Langmuir,* **2007**, *23*, 5787.

[15] Ratheesh Kumar, V. K.; Gopidas, K. R. Synthesis and characterization of gold-nanoparticle-cored dendrimers stabilized by metal-carbon bonds. *Chemistry - An Asian Journal,* **2010**, *5*, 887-896.

[16] Yan, H.; Wong, C.; Chianese, A. R.; Luo, J.; Wang, L.; Yin, J.; Zhong, C.-J. Dendritic Arenethiol-Based Capping Strategy for Engineering Size and Surface Reactivity of Gold Nanoparticles. *Chemistry of Materials,* **2010**, *22*, 5918.

[17] Love, J. C.; Estroff, L. A.; Kriebel, J. K.; Nuzzo, R. G.; Whitesides, G. M. Self-assembled monolayers of thiolates on metals as a form of nanotechnology. *Chemical Reviews,* **2005**, *105*, 1103-1169.

[18] Badia, A.; Lennox, R. B.; Reven, L. A Dynamic View of Self-Assembled Monolayers. *Accounts of Chemical Research,* **2000**, *33*, 475-481.

[19] Badia, A.; Gao, W.; Singh, S.; Demers, L.; Cuccia, L.; Reven, L. Structure and Chain Dynamics of Alkanethiol-Capped Gold Colloids. *Langmuir,* **1996**, *12*, 1262-1269.

[20] Chechik, V.; Schönherr, H.; Vancso, G. J.; Stirling, C. J. M. Self-assembled monolayers of branched thiols and bisulfides on gold: Surface coverage, order and chain orientation. *Langmuir,* **1998**, *14*, 3003-3010.

[21] Paez, J. I.; Coronado, E. A.; Strumia, M. C. Preparation of Controlled Gold Nanoparticle Aggregates using a Dendronization Strategy. *Journal of Colloid and Interface Science,* **2012**, *384* 10-21

[22] Note that although it has been proposed that the disulfide moiety is cleaved and two S-Au bonds are formed, it is also possible the occurrence of sulfur atoms bound to one and two gold atoms.

[23] Jiang, G.; Wang, L.; Chen, T.; Yu, H.; Chen, C. Preparation of gold nanoparticles in the presence of poly(benzyl ether) alcohol dendrons. *Materials Chemistry and Physics,* **2006**, *98*, 76-82.

[24] Hostetler, M. J.; Wingate, J. E.; Zhong, C. J.; Harris, J. E.; Vachet, R. W.; Clark, M. R.; Londono, J. D.; Green, S. J.; Stokes, J. J.; Wignall, G. D.; Glish, G. L.; Porter, M. D.; Evans, N. D.; Murray, R. W. Alkanethiolate gold cluster molecules with core diameters from 1.5 to 5.2 nm: Core and monolayer properties as a function of core size. *Langmuir,* **1998**, *14*, 17-30.

[25] Wang, R.; Yang, J.; Zheng, Z.; Carducci, M. D.; Jiao, J.; Seraphin, S. Dendron-controlled nucleation and growth of gold nanoparticles. *Angewandte Chemie - International Edition,* **2001**, *40*, 549-552.

[26] González De Rivera, F.; Rodríguez, L. I.; Rossell, O.; Seco, M.; Divins, N. J.; Casanova, I.; Llorca, J. Carbosilane dendrons as stabilizing agents for the formation of gold nanoparticles. *Journal of Organometallic Chemistry,* **2011**, *696*, 2287-2293.

[27] Nakao, S.; Torigoe, K.; Kon-No, K.; Yonezawa, T. Self-assembled one-dimensional arrays of gold-dendron nanocomposites. *Journal of Physical Chemistry B,* **2002**, *106*, 12097.

[28] Wu, L.; Li, B.-L.; Huang, Y.-Y.; Zhou, H.-F.; He, Y.-M.; Fan, Q.-H. Phosphine Dendrimer-Stabilized Palladium Nanoparticles, a Highly Active and Recyclable Catalyst for the Suzuki-Miyaura Reaction and Hydrogenation. *Organic Letters,* **2006**, *8*, 3605-3608.

[29] Yang, P.; Zhang, W.; Du, Y.; Wang, X. Hydrogenation of nitrobenzenes catalyzed by platinum nanoparticle core-polyaryl ether trisacetic acid ammonium chloride dendrimer shell nanocomposite. *Journal of Molecular Catalysis A: Chemical,* **2006**, *260*, 4-10.

[30] Porter Jr, L. A.; Ji, D.; Westcott, S. L.; Graupe, M.; Czernuszewicz, R. S.; Halas, N. J.; Lee, T. R. Gold and silver nanoparticles functionalized by the adsorption of dialkyl disulfides. *Langmuir,* **1998**, *14*, 7378-7386.

[31] Srisombat, L.-o.; Park, J.-S.; Zhang, S.; Lee, T. R. Preparation, Characterization, and Chemical Stability of Gold Nanoparticles Coated with Mono-, Bis-, and Tris-Chelating Alkanethiols. *Langmuir,* **2008**, *24*, 7750-7754.

[32] Paulini, R.; Frankamp, B. L.; Rotello, V. M. Effects of Branched Ligands on the Structure and Stability of Monolayers on Gold Nanoparticles. *Langmuir,* **2002**, *18*, 2368-2373.

[33] Daniel, M.-C.; Grow, M. E.; Pan, H.; Bednarek, M.; Ghann, W. E.; Zabetakis, K.; Cornish, J. Gold nanoparticle-cored poly(propyleneimine) dendrimers as a new platform for multifunctional drug delivery systems. *New Journal of Chemistry,* **2012**, *35*, 2366-2374.

[34] Clegg, R. S.; Hutchison, J. E. Hydrogen-bonding, self-assembled monolayers: Ordered molecular films for study of through-peptide electron transfer. *Langmuir,* **1996**, *12*, X-5243.

[35] Tam-Chang, S. W.; Biebuyck, H. A.; Whitesides, G. M.; Jeon, N.; Nuzzo, R. G. Self-assembled monolayers on gold generated from alkanethiols with the structure $RNHCOCH_2SH$. *Langmuir,* **1995**, *11*, 4371-4382.

[36] Cai, S.; Singh, B. R. A Distinct Utility of the Amide III Infrared Band for Secondary Structure Estimation of Aqueous Protein Solutions Using Partial Least Squares Methods. *Biochemistry,* **2004**, *43*, 2541-2549.

[37] Pietsch, T.; Appelhans, D.; Gindy, N.; Voit, B.; Fahmi, A. Oligosaccharide-modified dendrimers for templating gold nanoparticles: Tailoring the particle size as a function of dendrimer generation and -molecular structure. *Colloids and Surfaces A: Physicochemical and Engineering Aspects,* **2009**, *341*, 93.

[38] Silverstein, R. M.; Webster, F. X.; Kiemle, D. *Spectrometric Identification of Organic Compounds*; 7th ed.; John Wiley & Sons, 2005.

[39] Hasan, M.; Bethell, D.; Brust, M. The fate of sulfur-bound hydrogen on formation of self-assembled thiol monolayers on gold: ^1H NMR spectroscopic evidence from solutions of gold clusters. *Journal of the American Chemical Society,* **2002**, *124*, 1132-1133.

[40] Templeton, A. C.; Wuelfing, W. P.; Murray, R. W. Monolayer-protected cluster molecules. *Accounts of Chemical Research,* **2000**, *33*, 27-36.

[41] Ingram, R. S.; Hostetler, M. J.; Murray, R. W. Poly-hetero-ω-functionalized Alkanethiolate-stabilized gold cluster compounds. *Journal of the American Chemical Society,* **1997**, *119*, 9175-9178.

[42] Shon, Y. S.; Choi, D.; Dare, J.; Dinh, T. Synthesis of nanoparticle-cored dendrimers by convergent dendritic functionalization of monolayer-protected nanoparticles. *Langmuir,* **2008**, *24*, 6924.

[43] Pérez, Y.; Mann, E.; Herradón, B. Preparation and characterization of gold nanoparticles capped by peptide-biphenyl hybrids. *Journal of Colloid and Interface Science,* **2011**, *359*, 443-453.

[44] Chiang, C. L. Controlled growth of gold nanoparticles in AOT/C12E4/isooctane mixed reverse micelles. *Journal of Colloid and Interface Science,* **2001**, *239*, 334-341.

[45] Luty-Blocho, M.; Fitzner, K.; Hessel, V.; Löb, P.; Maskos, M.; Metzke, D.; Paclawski, K.; Wojnicki, M. Synthesis of gold nanoparticles in an interdigital micromixer using ascorbic acid and sodium borohydride as reducers. *Chemical Engineering Journal,* **2011**, *171*, 279-290.

[46] Wu, Z.; MacDonald, M. A.; Chen, J.; Zhang, P.; Jin, R. Kinetic control and thermodynamic selection in the synthesis of atomically precise gold nanoclusters. *Journal of the American Chemical Society,* **2011**, *133*, 9670-9673.

[47] Gopidas, K. R.; Whitesell, J. K.; Fox, M. A. Synthesis, Characterization, and Catalytic Applications of a Palladium-Nanoparticle-Cored Dendrimer. *Nano Letters,* **2003**, *3*, 1757-1760.